



ELSEVIER

Available online at [www.sciencedirect.com](http://www.sciencedirect.com)SCIENCE @ DIRECT<sup>®</sup>

C. R. Chimie 8 (2005) 933–955

<http://france.elsevier.com/direct/CRAS2C/>

## Account / Revue

# Salts of a sandwich-type bis 9-tungstoarsenate(III) tris(oxorhenate(V)) polyoxoanion as precursors to tungsten–rhenium bronzes

Alexei Besserguenev, Michael T. Pope \*

*Department of Chemistry, Box 571227, Georgetown University, Washington, DC 20057-1227, USA*

Received 21 July 2004; accepted after revision 7 October 2004

Available online 03 February 2005

Dedicated to Professor Francis Sécheresse on the occasion of his 60th birthday

---

**Abstract**

Potassium and ammonium salts of the tungstoarsenate anion  $[(\text{Re}^{\text{V}}\text{O})_3(\text{AsW}_9\text{O}_{33})_2]^{9-}$  (**1**) have been isolated and characterized by elemental analysis, infrared and  $^{183}\text{W}$  NMR spectroscopy. The five-line NMR spectrum indicates a sandwich structure of  $C_{2v}$  symmetry analogous to that found for  $[\text{As}_2\text{W}_{21}\text{O}_{69}(\text{H}_2\text{O})]^{6-}$ . Thermal treatment of both salts of **1** at temperatures to 900 °C leads to materials in which ~95% of the rhenium is retained, in contrast to the Keggin-derived  $\text{K}_4\text{PW}_{11}\text{ReO}_{40}$  which loses rhenium at ~500 °C. Based upon powder diffraction analysis, following quantitative loss of  $\text{As}_2\text{O}_3$  at 420–430 °C, the following phases were identified in samples heated to 600 and 725 °C. From the potassium salt, a monoclinic  $\text{K}_2\text{W}_3\text{O}_{10}$ -type bronze, and from the ammonium salt a mixture of hexagonal and tetragonal  $\text{WO}_3$  bronzes. Reflections corresponding to  $\text{ReO}_2$ ,  $\text{ReO}_3$ , solid solutions of  $\text{ReO}_3$  in  $\text{WO}_3$ , and  $\text{Re}_2\text{O}_7$  were absent. The incorporation of rhenium into tungsten bronze phases suggests that technetium might behave similarly, opening a possible route to storage of  $^{99}\text{Tc}$  waste. **To cite this article:** A. Besserguenev, M.T. Pope, *C. R. Chimie* 8 (2005).

© 2005 Académie des sciences. Published by Elsevier SAS. All rights reserved.

**Résumé**

**Les sels d'un sandwich-type bis 9-tungstoarsenate(III) tris(oxorhenate(V)) polyoxoanion en tant que précurseurs des bronzes tungstène–rhénium.** Les sels de potassium et ammonium de l'anion tungstoarsenate(III)  $[(\text{Re}^{\text{V}}\text{O})_3(\text{AsW}_9\text{O}_{33})_2]^{9-}$  (**1**) ont été isolés et caractérisés par analyse élémentaire, spectroscopie infrarouge et  $^{183}\text{W}$  RMN. Le spectre RMN cinq lignes indique une structure sandwich de symétrie  $C_{2v}$  analogue à la structure connue de  $[\text{As}_2\text{W}_{21}\text{O}_{69}(\text{H}_2\text{O})]^{6-}$ . Le traitement thermique des sels de **1** aux températures jusqu'à 900 °C conduit à des matériaux qui conservent 95% de leur contenu en rhénium, contrairement à  $\text{K}_4\text{PW}_{11}\text{ReO}_{40}$ , de structure Keggin, qui perd son rhénium à ~500 °C. Sur la base de l'analyse par diffraction sur poudre, les phases suivantes ont été identifiées dans les échantillons chauffés à 600 et 725 °C après perte quantitative de  $\text{As}_2\text{O}_3$  à 420–430 °C. On a obtenu, à partir du sel de potassium, un bronze monoclinique de type  $\text{K}_2\text{W}_3\text{O}_{10}$  et, à partir du sel d'ammonium,

---

\* Corresponding author.E-mail address: [popem@georgetown.edu](mailto:popem@georgetown.edu) (M.T. Pope).

un mélange de bronzes  $\text{WO}_3$  hexagonaux et tétraugonaux. Les réflexions correspondant à  $\text{ReO}_3$ , à  $\text{ReO}_2$ , aux solutions solides de  $\text{ReO}_3/\text{WO}_3$  et à  $\text{Re}_2\text{O}_7$  étaient absentes. L'incorporation du rhénium dans les phases de tungstène suggère que le technétium se comporte de la même façon, qui ouvrant une possible voie au stockage des déchets de  $^{99}\text{Tc}$ . **Pour citer cet article :** A. Besserguenev, M. T. Pope, C. R. Chimie 8 (2005).

© 2005 Académie des sciences. Published by Elsevier SAS. All rights reserved.

**Keywords:** Polyoxometalates; Tungsten; Rhenium; Tungsten bronzes

**Mots clés :** Polyoxometallates ; Tungstène ; Rhénium ; Bronzes de tungstène

## 1. Introduction

The use of polyoxometalates [1–4] as potential sequestering agents and/or as sources of storage matrices ('waste forms') for radioactive waste has attracted attention for several years. One particularly troubling isotope is technetium-99 with a half-life of  $\sim 10^5$  years that is readily transformed to the volatile heptaoxide during the vitrification processes currently envisioned for production of waste forms, or is converted to soluble pertechnetates that have high mobility in ground waters. We have recently been investigating the potentialities of polyoxometalates for the technetium problem, using in the first instance rhenium as a non-radioactive surrogate [5]. In related studies we have shown that tungsten bronzes incorporating lanthanide and actinide ions are efficiently produced by thermal decomposition at relatively low temperatures of the corresponding polyoxotungstate complexes [6]. The inertness of tungsten bronzes make them possible attractive targets for waste forms.

With the exception of hexametalate-supported triscarbonylrhenium(I) complexes prepared under non-aqueous [7] or aqueous [5] conditions, previously-characterized rhenium-containing polyoxometalates incorporate rhenium, usually in oxidation state V, in place of one or two tungsten(VI) atoms in Keggin [8], Wells-Dawson [9] or decatungstate [10] structures. Examples of analogous technetium(V) Keggin derivatives have also been described [11].

We report here the synthesis and characterization of a new type of tungstorhenate derivative with relatively high rhenium content ( $\text{Re}/\text{W} = 1:6$ ). Thermal decomposition of potassium and ammonium salts of the new complex does not result in loss of rhenium at temperatures up to  $900^\circ\text{C}$ , and leads to new tungsten–rhenium bronzes.

## 2. Experimental

### 2.1. Syntheses

Potassium pentachloro(oxo)rhenate(V) was prepared by reduction of 55% perrhenic acid (Alfa Aesar) with hydriodic acid according to the method of Ivanov-Emin et al. [12]. Isolated yield, 60%; IR,  $940\text{ cm}^{-1}$  ( $\text{Re}=\text{O}$ ). Potassium and ammonium salts of  $[\text{PW}_{11}\text{O}_{39}]^{7-}$  were isolated from stoichiometric mixtures of  $\text{PO}_4^{3-}$  and  $\text{WO}_4^{2-}$  adjusted to pH 5.2 and their identities confirmed by  $^{31}\text{P}$ -NMR and IR. Sodium 9-tungstoarsenate(III),  $\text{Na}_9\text{AsW}_9\text{O}_{33}\cdot n\text{H}_2\text{O}$  ( $\text{AsW}_9$ ) was prepared according to the literature [13]. IR, 935(vs), 898(vs), 783(vs), 727(vs), 515(w), 472(w), 443(w), 411(w)  $\text{cm}^{-1}$ .

The potassium salt of  $[(\text{ReO})_3(\text{AsW}_9\text{O}_{33})_2]^{9-}$  (**K-1**) was prepared as follows. Potassium pentachloro(oxo)rhenate(V) ( $\text{K}_2\text{ReOCl}_5$ , 0.67 g, 1.5 mmol) was added to a solution of potassium thiocyanate (KSCN, 1.95 g, 20 mmol) in 20 ml of deoxygenated water. After the rhenium complex had dissolved completely, sodium perchlorate ( $\text{NaClO}_4$ , 3.04 g) was added and the mixture was cooled to  $5^\circ\text{C}$  in an ice bath. A white precipitate of potassium perchlorate was filtered off. Sodium 9-tungstoarsenate(III) (2.74 g, 1 mmol) was added to the solution of the rhenium(V) complex. The color of the reaction mixture color changed from green to red-brown and the mixture was stirred for 30 min at room temperature. Any undissolved  $\text{AsW}_9$  was filtered off. Saturated potassium chloride solution (20 ml) was added to the reaction mixture and it was cooled to  $5^\circ\text{C}$  in an ice bath. A dark brown precipitate (1.15 g, 40%) was filtered off and suction dried. Anal. Found (Calc. for  $\text{K}_9[(\text{ReO})_3(\text{AsW}_9\text{O}_{33})_2]\cdot 23\text{ H}_2\text{O}$ ): K 6.1 (6.0), Na 0.3 (0), Re 9.76 (9.49), As 2.57 (2.54), W 56.1 (56.2). An ammonium salt (**NH<sub>4</sub>-1**) was prepared similarly.

The product (yield 0.85 g, 30%) was precipitated by addition of 20 ml of 5 M  $(\text{NH}_4)\text{Cl}$ .

The water-soluble potassium salt of  $[\text{PW}_{11}\text{ReO}_{40}]^{4-}$  (' $\text{PW}_{11}\text{Re}$ '), previously only known as a tetra-*n*-butylammonium salt [8], was prepared by dissolving  $\text{K}_7\text{PW}_{11}\text{O}_{39} \cdot 15 \text{ H}_2\text{O}$ , (6.44 g, 2 mmol) in 60 ml of a 0.06 M-acetate buffer (pH 4) that had been deaerated with a stream of nitrogen for 30 min. The solution was heated to 50 °C and the  $\text{K}_2\text{ReOCl}_5$  (0.92 g, 2 mmol) was added. The reaction mixture was heated at 50 °C under a nitrogen atmosphere for 1.5 h. Saturated potassium chloride solution (80 ml) was added and the resulting purple precipitate (1.45 g) was filtered off.  $^{31}\text{P}$ -NMR showed an impurity (probably unreacted  $\text{PW}_{11}$ ) at -10.9 ppm, as well as the major product at -15.1 ppm. The product was dissolved in 40 ml of deaerated water; the suspension was heated to ~50 °C until the solid dissolved completely and saturated potassium chloride solution was added and the mixture cooled to 5 °C in an ice bath. The precipitate (1.29 g, 21%) was collected and suction dried. The procedure was repeated two times until only one peak (-15.1 ppm) was observed in the  $^{31}\text{P}$ -NMR spectrum. Tungsten-183 NMR:  $\delta/\text{ppm}$  (relative intensity): -99 (2), -115 (2), -116 (1), -207 (2), -274 (2), -290 (2).

## 2.2. Instrumental

Infrared spectra were measured on a Nicolet 7000 spectrometer from 4000 to 400  $\text{cm}^{-1}$  with resolution of 2  $\text{cm}^{-1}$ . All samples were prepared as KBr pellets. Thermogravimetric analysis (TGA) curves were obtained on a TGA 2050 analyzer (TA Instruments) from room temperature to 950 °C under a nitrogen atmosphere. Alumina pans were used for all experiments. Differential scanning calorimetry (DSC) was recorded on a DSC 2910 calorimeter (TA Instruments) from room temperature to 725 °C under a nitrogen atmosphere. Platinum pans were used for all measurements. Cyclic voltammetry was performed on a BAS 100A electrochemical analyzer using a glassy carbon working electrode and platinum counter electrode using a sweep rate of 500 mV s<sup>-1</sup>. Potentials are reported with respect to a Ag/AgCl reference electrode.

NMR spectra were recorded on Bruker AM 300 ( $^{31}\text{P}$ ,  $^{183}\text{W}$ ) or Varian Mercury 300 ( $^{31}\text{P}$ ) spectrometers. Typical parameters for phosphorus-31 NMR spectra were: offset frequency, 121.497 MHz; bandwidth, 3650 Hz

and repetition rate, 0.6 Hz. Chemical shifts were measured relative to 85% phosphoric acid. Typical parameters for  $^{183}\text{W}$  NMR spectra were: offset frequency, 12.504 MHz; bandwidth, 5 KHz and repetition rate, 0.4 Hz. Chemical shifts were measured relative to 2 M  $\text{Na}_2\text{WO}_4$ . For collection of  $^{183}\text{W}$ -NMR spectra potassium salts of  $\text{PRe}^{\text{V}}\text{W}_{11}$  and **1** were exchanged to lithium salts using lithium perchlorate ( $\text{LiClO}_4$ ). For the exchange, 1–2 g of the polyoxometalate sample, a stoichiometric amount of  $\text{LiClO}_4$  and 2 ml of  $\text{D}_2\text{O}$  were mixed together and stirred for 30 min. Insoluble  $\text{KClO}_4$  was filtered off and the filtrate was used to collect the NMR spectrum.

Powder diffraction patterns were collected on a RIGAKU R-Axis Rapid XRD automated powder diffractometer equipped with an Image Plate detector. For a typical sample preparation, fine powder was mixed with vaseline and the mixture was smeared onto the surface of a single crystal silicon sample holder. The data were collected in reflection geometry and were integrated using the RIGAKU R-Axis Rapid XRD software package, producing diffraction intensity vs.  $2\theta$  diffraction angle dependencies. These were processed using the Materials Data Jade 5.0 XRD software package. Final processing using Jade included background subtraction and peak search. Phase identification was performed by comparing peaks found with powder diffraction patterns of pure compounds stored in the database provided with the Jade software package.

## 3. Results and discussion

### 3.1. Synthesis and characterization of **1**

Since several examples of sandwich complexes of the type  $[\text{M}_3(\text{AsW}_9\text{O}_{33})_2]^{12-}$  (e.g. with  $\text{M} = \text{Mn}(\text{H}_2\text{O})$ ,  $\text{Co}(\text{H}_2\text{O})$ ,  $\text{Ni}(\text{H}_2\text{O})$ ,  $\text{VO}^{2+}$ ,  $\text{WO}^{4+}$ ) are known [14,15], reaction of  $\{\text{ReO}^{3+}\}$  and  $\text{AsW}_9$  in a 3:2 molar ratio proceeds straightforwardly. It is necessary, however, to prevent rapid hydrolysis of  $[\text{ReOCl}_5]^{2-}$  in aqueous solution by complexation with excess thiocyanate, and to exchange sodium for potassium in the resulting solution to allow for ready subsequent dissolution of  $\text{AsW}_9$ . Although crystals suitable for X-ray structural determination have not yet been obtained, there is little doubt about the composition and structure of **1**. The molecular formula is supported by elemental analysis of the

potassium salt and the infrared spectrum in the metal–oxygen stretching region is virtually identical to that of  $\text{Na}_9\text{AsW}_9\text{O}_{33}$  indicating the presence of  $\text{AsW}_9$  building blocks. The  $^{183}\text{W}$  NMR spectrum of **1** shows five lines of relative intensity 1:2:2:2:2 at –79, –95, –102, –134, and –145 ppm, respectively, instead of the anticipated two lines for a complex of  $D_{3h}$  symmetry. This result implies that the three sandwiched  $\text{ReO}^{3+}$  groups are arranged with one  $\text{Re–O}$  vector directed towards the interior of the anion and the other two directed outwards, i.e. in similar fashion to the corresponding  $\text{WO}^{4+}$  groups in  $[\text{As}_2\text{W}_{21}\text{O}_{69}(\text{H}_2\text{O})]^{6-}$  ( $\equiv [\text{H}_2\text{O}(\text{WO})_3(\text{AsW}_9\text{O}_{33})_2]^{6-}$ ) to give a structure of  $C_{2v}$  symmetry, see Fig. 1. The presence of an ‘external’ water ligand in **1** cannot be confirmed in the absence of a crystal structure, although it seems probable.

In contrast to the Keggin-derived rhenium derivatives which display a rich electrochemical behavior corresponding to  $\text{Re(V)}-\text{Re(VI)}$  and  $\text{Re(VI)}-\text{Re(VII)}$  couples [8], cyclic voltammograms of **1** show only an irreversible anodic feature at +1.1 V vs.  $\text{Ag}/\text{AgCl}$ . We

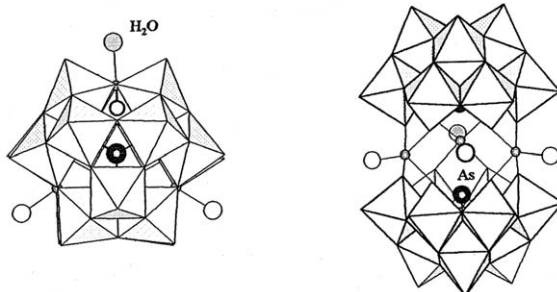
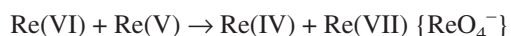


Fig. 1. Two polyhedral representations of the structure of  $[\text{As}_2\text{W}_{21}\text{O}_{69}(\text{H}_2\text{O})]^{6-}$  [15] showing the reduction in symmetry from  $D_{3h}$  to  $C_{2v}$  caused by the orientation of the equatorial  $\text{WO}^{4+}$  groups. Small gray spheres, W; open circles, terminal oxygens; gray circle, water ligand. An analogous structure with equatorial  $\text{ReO}^{3+}$  groups is proposed for **1**.

presume that the proximity of the rhenium centers in **1** allows facile electron transfer and effective disproportionation of any  $\text{Re(VI)}$ , e.g. via



Attempts to oxidize **1** by addition of bromine water led to immediate decolorization.

### 3.2. Thermal decomposition of **1**

We have previously shown that ammonium salts of polyoxotungstates containing lanthanide and actinide heteroatoms may be thermally decomposed to yield cubic tungsten bronzes that might be suitable as waste forms for lanthanide and actinide radioisotopes [6]. We, therefore, decided to explore the thermal behavior of rhenium-containing polytungstates as models for the corresponding technetium species. Several years ago Sleight and Gillson [16] had investigated solid solutions of  $\text{WO}_3$  and  $\text{ReO}_3$ , which are isoelectronic with the cubic bronzes  $\text{M}_x\text{WO}_3$ .

Comparative thermogravimetric scans of  $\text{K}_4[\text{PW}_{11}\text{ReO}_{40}]$  and  $\text{K}_3[\text{PW}_{12}\text{O}_{40}]$  revealed that the former salt lost its rhenium content, presumably as  $\text{Re}_2\text{O}_7$ , at temperatures above 500 °C. In contrast both **K-1** and  $\text{NH}_4\text{-1}$  yielded mixed rhenium–tungsten bronzes. Fig. 2 shows the TGA and DSC results for these two salts. Following loss of crystal water below 200 °C for both salts and volatilization of  $\text{NH}_3$  by 400 °C. The exothermic DSC peaks at 417 °C (**K**) and 433 °C ( $\text{NH}_4$ ) correspond to weight losses of 3.56% and 3.88%, respectively, attributed to the decomposition of the anion via loss of  $\text{As}_2\text{O}_3$  (ca. 3.33% and 3.46%). No other significant weight loss was observed up to 950 °C. Between 600 and 950 °C the sample lost 0.31% ( $\text{NH}_4$ ) 1.1% (**K**) of its initial weight, indicating that most of the rhenium was still left in the sample.

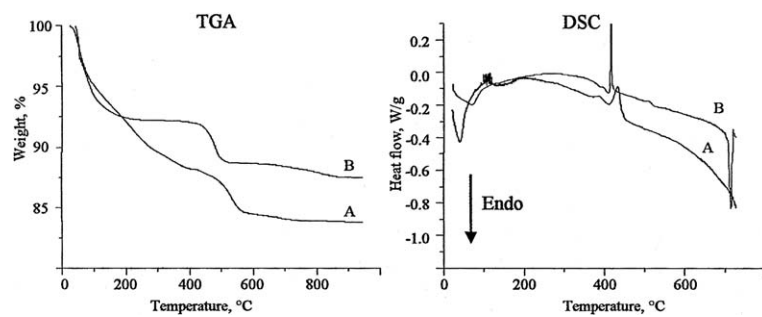


Fig. 2. TGA and DSC curves of  $(\text{NH}_4)_9[(\text{ReO})_3(\text{AsW}_9\text{O}_{33})_2]\cdot n\text{H}_2\text{O}$  (A) and  $\text{K}_9[(\text{ReO})_3(\text{AsW}_9\text{O}_{33})_2]\cdot n\text{H}_2\text{O}$ .

Elemental analysis of the ammonium salt heated to 950 °C in the TGA apparatus indicated that ~95% of the rhenium was left in the sample after heating. Anal. (Calc. for 1.5(Re<sub>2</sub>O<sub>5</sub>):18(WO<sub>3</sub>): Re 10.89 (11.51); W 67.7 (68.2).

Phase identification in the samples of potassium and ammonium salts of **1** was carried out using powder diffraction. Analysis of powder diffraction patterns of the potassium salt samples decomposed at 600 and 725 °C (Fig. 3) indicates the presence of a monoclinic compound similar to potassium tritungstate, K<sub>2</sub>W<sub>3</sub>O<sub>10</sub> (Fig. 4) [17]. Most of the observed diffraction peaks correspond to the powder diffraction pattern of

K<sub>2</sub>W<sub>3</sub>O<sub>10</sub>. Observed differences in intensities of two low-angle peaks result from obstruction by the sample holder and absorption of diffracted rays by cavities on the real (not smooth) surface of the sample. Some peaks, which were not found in the diffraction pattern of K<sub>2</sub>W<sub>3</sub>O<sub>10</sub> could be still indexed on the basis of the K<sub>2</sub>W<sub>3</sub>O<sub>10</sub> monoclinic unit cell (see Section 5, Tables S1 and S2). Four reflections which could not be indexed on the basis of the K<sub>2</sub>W<sub>3</sub>O<sub>10</sub> monoclinic cell do not correspond to any of the known rhenium oxides: ReO<sub>2</sub> [18], ReO<sub>3</sub> [19], Re<sub>2</sub>O<sub>7</sub> [20] or to the ReO<sub>3</sub>–WO<sub>3</sub> solid solutions [16]. The unit cell constants of the monoclinic cell were refined based on the assigned Miller

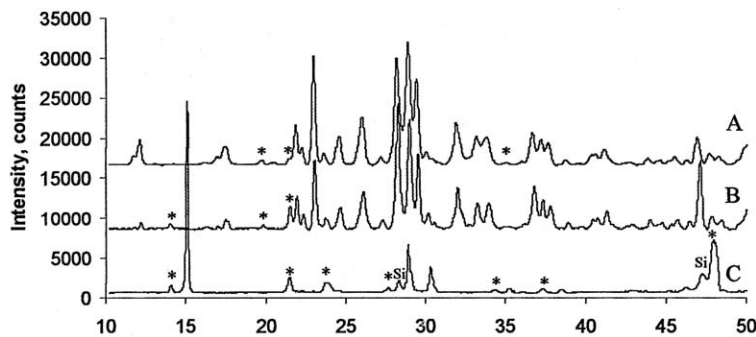


Fig. 3. Powder diffractograms of samples of K<sub>9</sub>[(ReO<sub>3</sub>)(AsW<sub>9</sub>O<sub>33</sub>)<sub>2</sub>]·n H<sub>2</sub>O, heated to 600 °C (A), 725 °C (B), and 900 °C (C). (\*) Unidentified reflections. (Si) reflections from silicon sample holder.

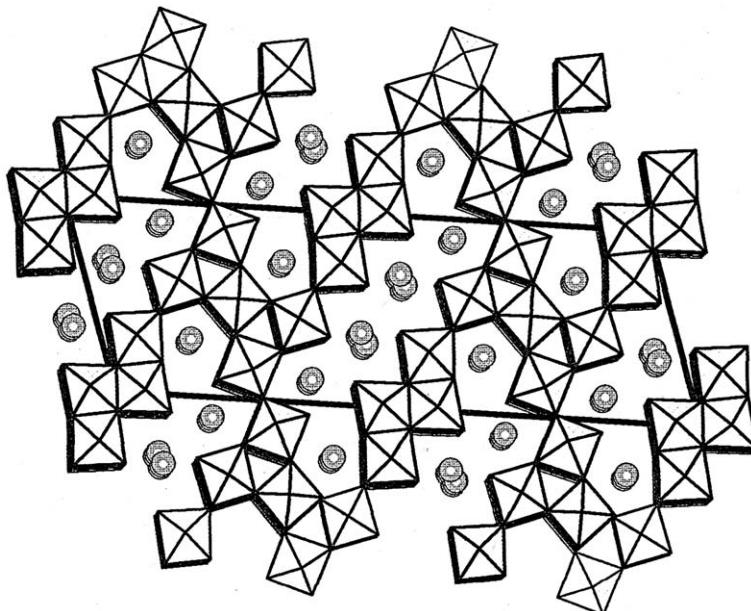


Fig. 4. Monoclinic K<sub>2</sub>W<sub>3</sub>O<sub>10</sub> structure. Crystallographic *b*-axis perpendicular to the plane of paper. Potassium cations (gray spheres) occupy positions in the large channels formed by tungsten oxide framework.

Table 1

Phase composition of ammonium and potassium salts of  $[(\text{ReO})_3(\text{AsW}_9\text{O}_{33})_2]^{9-}$  following thermal degradation

Decomposition temperature (°C)	K-salt	(NH <sub>4</sub> )-salt
600	Potassium bronze ( $\text{K}_2\text{W}_3\text{O}_{10}$ -type): $a = 10.91(2)$ Å, $b = 3.881(4)$ Å, $c = 15.97(2)$ Å, $\beta = 109.0(1)^\circ$	Mixture of two phases: hexagonal bronze: $a = 7.324(7)$ Å, $c = 7.519(7)$ Å; tetragonal bronze: $a = 5.243(2)$ Å, $c = 3.879(1)$ Å
725	Potassium bronze ( $\text{K}_2\text{W}_3\text{O}_{10}$ -type): $a = 10.86(2)$ Å, $b = 3.866(5)$ Å, $c = 15.96(2)$ Å, $\beta = 109.0(1)^\circ$	Mixture of two phases: hexagonal bronze: $a = 7.2890(5)$ Å, $c = 7.5644(6)$ Å; tetragonal bronze: $a = 5.2457(9)$ Å, $c = 3.868(1)$ Å
900	Potassium bronze ( $\text{WO}_3 \cdot \frac{1}{2}\text{H}_2\text{O}$ pyrochlore-type): $a = 10.172(3)$ Å	Mixture of two phases: hexagonal bronze: $a = 7.316(4)$ Å, $c = 7.545(3)$ Å; orthorhombic bronze: $a = 7.372(5)$ Å, $b = 7.499(5)$ Å, $c = 3.860(3)$ Å

indexes and are given in Table 1 (see Tables S7–S15 in Section 5). The refinement indicated no significant differences between unit cell parameters of samples heated to 600 and 725 °C.

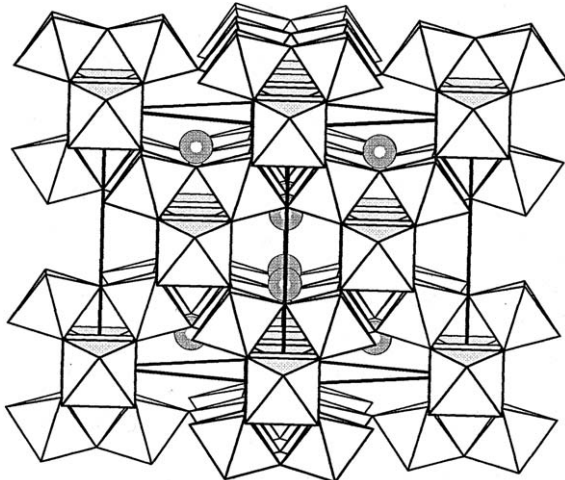


Fig. 5. Pyrochlore-type structure viewed perpendicular to the (110) plane, showing locations of potassium cations (gray spheres).

The powder diffraction pattern of the potassium salt heated to 900 °C differs significantly from the patterns collected for samples decomposed at lower temperatures. Since the TGA curve does not show any stepwise weight loss between 725 and 950 °C, the observed change of phase composition suggests an existence of a phase transition in this temperature interval. A search on the powder diffraction database shows that the observed powder diffraction pattern corresponds to those of hydrated tungsten oxide  $\text{WO}_3 \cdot 0.5\text{H}_2\text{O}$  and a number of substituted tungsten bronzes,  $\text{KCr}_{0.33}\text{W}_{1.67}\text{O}_6$  with pyrochlore-type structures (Fig. 5; Section 5, Table S3) [21].

A rough estimate of the rhenium contribution to the intensity of diffraction, based on the formula of the decomposed product, shows that rhenium should contribute about  $\{3(\text{Re})/[18(\text{W}) + 8 \times 69(\text{O})/74 + 19 \times 9(\text{K})/74]\} \times 100\% \approx 11\%$  of total diffraction intensity. The intensities of the unidentified peaks increase with increase of temperature, for example, the reflection with  $d = 4.13$  Å increases from 5.9% at 600 °C to 18% at

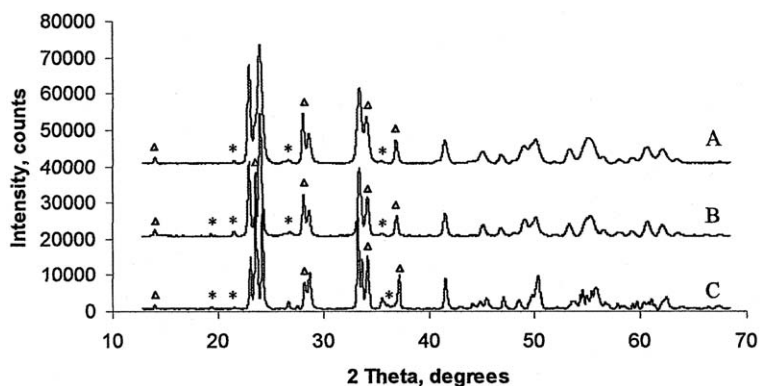


Fig. 6. Powder diffractograms of  $(\text{NH}_4)_9[(\text{ReO})_3(\text{AsW}_9\text{O}_{33})_2] \cdot n\text{H}_2\text{O}$  heated to 600 °C (A), 725 °C (B), and 900 °C. (\*) Unidentified reflections. (Δ) Reflections from the hexagonal phase.

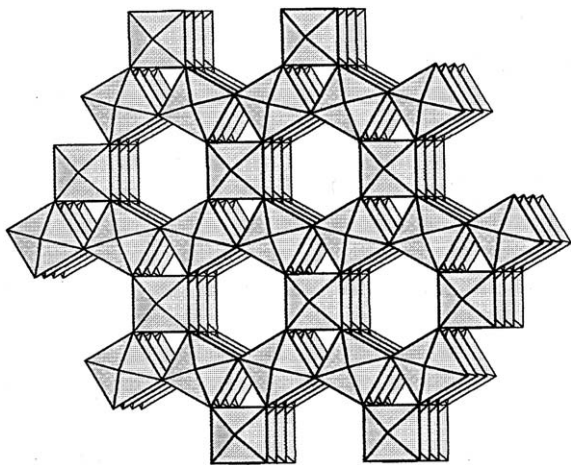


Fig. 7. Structure of hexagonal tungsten bronze (oxide) showing the channels parallel to the crystallographic *c*-axis.

725 and 900 °C, which probably indicates decomposition of the monoclinic phase and formation of a cubic phase. At 600 °C, according to this estimate, a considerable part of the rhenium should be in the monoclinic phase, but it is unclear how much rhenium, if any is contained in the monoclinic, or cubic phase at the higher temperature.

A powder diffraction study of decomposition products resulting from heating the ammonium salt of **1** to 725 °C, shows two different crystallographic phases corresponding to hexagonal [22,23] and tetragonal [24] bronzes (Fig. 6, Tables 1, S4 and S5). As for the potas-

sium salt a few low-intensity reflections could not be identified as known rhenium oxides and bronzes [18,20–22,25], or indexed in either tetragonal [24] or hexagonal [22,23] cell settings. A rough estimate of the rhenium contribution to the intensity of diffraction on the basis of decomposition product's formula:  $\text{Re}_{1.9}\text{W}_{12}\text{O}_{41}$  suggests that rhenium should contribute about:  $\{2(\text{Re})/[12(\text{W}) + 8 \times 41(\text{O})/74]\} \times 100\% \approx 12\%$  of observed diffraction intensity, which is about three times greater than the most intense non-identified peak: 3.9% (Tables S4 and S5). This estimate suggests that considerable part of rhenium is incorporated into the observed tetragonal and hexagonal phases.

The hexagonal bronze structure is formed of  $\text{WO}_6$  octahedra connected by vertices (Fig. 7). Cations reside inside the large channels. The hexagonal structural framework is stable even if channels are empty, so that a hexagonal tungsten oxide ( $\text{WO}_3$ ) structure exists [22,23]. The tetragonal bronze structure is similar to the structure of perovskite [24,25]. The perovskite structure consists of a framework of  $\text{WO}_6$  octahedra connected by vertices (Fig. 8). This forms a cubic-type 3D structure, with interconnected pores partially occupied by cations. Since the tungsten octahedra are distorted, there is a deviation from ideal cubic symmetry. The *a*-axis of the smallest tetragonal cell is equal to the face diagonal of the cubic cell ( $a = 3.8 \times \sqrt{2} \approx 5.22 \text{ \AA}$ ). Some tetragonal bronzes have been indexed on the basis of a larger tetragonal cell with  $a \sim 7.4 \text{ \AA}$ , which approxi-

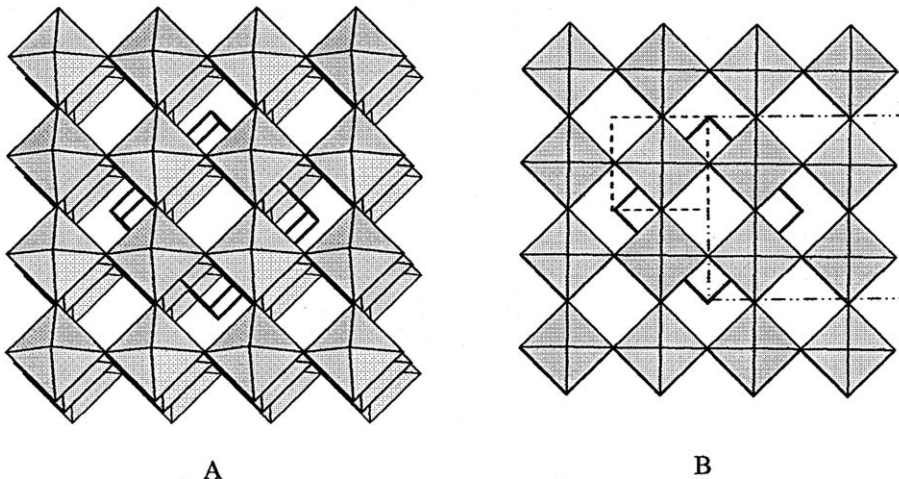


Fig. 8. Structure of tetragonal tungsten bronze (oxide). A, a perspective along the *c*-axis. B, relationship between different lattice cell types. Perovskite-type cubic cell ( $a \sim 3.7 \text{ \AA}$ ) is shown by dashed line; smallest tetragonal cell ( $a \sim 5.2 \text{ \AA}$ ) is shown by continuous line; larger tetragonal cell ( $a \sim 7.4 \text{ \AA}$ ) is shown by another type of dashed line. Crystallographic *c*-axis is perpendicular to the plane of paper.

mately equals  $2a$  for the cubic cell (Fig. 8). For both tetragonal cell types  $c$  (~3.8 Å) is close to the parameter for the cubic cell. Structures with orthorhombic or monoclinic symmetry with unit cells close to the larger tetragonal cell have also been reported [26,27]. Decomposition products found at 600 and 725 °C could be indexed on the basis of both tetragonal cells with a cell parameter of either ~5.22 Å (' $\text{Ca}_{0.035}\text{WO}_3$ ') or ~7.4 Å (' $\text{H}_{0.23}\text{WO}_3$ '), which in fact represent the same perovskite-type structure.

Sleight and Gillson [16] studied formation of  $\text{WO}_3$ – $\text{ReO}_3$  solid solutions. They found cubic ( $a = 3.7574$  Å), perovskite-type phases, similar to the tetragonal (orthorhombic) phase observed for the decomposition of ammonium salt of **1**.

As for the potassium salt, a change in powder diffraction pattern was observed for a sample decomposed at 900 °C. Search of a match in the powder diffraction database shows a mixture of hexagonal (also observed at lower temperatures) and orthorhombic phases.

The lattice parameters of the orthorhombic compound are very similar to those of the tetragonal compound, suggesting a deformation of the tetragonal lattice. Orthorhombic deformation of a tetragonal lattice is easily demonstrated by splitting of the (1 1 0) reflection of the tetragonal phase (3.71, 100%, Tables S4 and S5) into the (0 2 0), (2 0 0) reflections of the orthorhombic phase (3.74, 38%; 3.67, 74%, Table S6).

Thus thermal decomposition of the ammonium salt of  $[(\text{ReO})_3(\text{AsW}_9\text{O}_{33})_2]^{9-}$  gives mostly a mixture of hexagonal and tetragonal (perovskite) type bronzes. The intensities of the diffraction peaks that belong to the

hexagonal phase increase with increasing temperature, which suggests higher stability of the hexagonal phase at high temperatures. A structural phase transition is observed for the tetragonal phase between 725 and 900 °C, which results in an orthorhombic deformation of the observed unit cell.

#### 4. Conclusions

Thermolysis of solid samples of ammonium and potassium salts of the new sandwich polyoxometalate anion  $[(\text{ReO})_3(\text{AsW}_9\text{O}_{33})_2]^{9-}$  at 600–900 °C yield tungsten–rhenium bronzes based on  $\text{K}_2\text{W}_3\text{O}_{10}$  and hexagonal and tetragonal oxides. About 95% of the rhenium content of the original polyoxoanion is retained at 900 °C. This behavior suggests the possibility of generating analogous thermally stable technetium oxide bronzes for use as radioactive waste forms.

#### Acknowledgments

We thank the DOE for support of this work through the Office of Energy research and Environmental Management Science Program, Grant DE-FG07-96ER14695.

#### Supporting information

Tables S1–S15 listing phase identification and unit cell refinement from powder diffractograms of thermally-treated samples of **1-K**, and **1-NH<sub>4</sub>**.

Table S1

Phase identification for a sample of  $K_9[(ReO)_3(AsW_9O_{33})_2] \cdot n H_2O$  heated to 600 °C in TGA apparatus under N<sub>2</sub> atmosphere

$2\theta$ (obs)	$d$ (obs) (Å)	$I$ (obs) (%)	Phase ID	$d$ (card) (Å)	$I$ (card) (%)	$h \ k \ l$	$2\theta$ (card)	$\Delta(2\theta)$
11.739	7.5323	8.8	$K_2W_3O_{10}$	7.5400	70.0	0 0 2	11.727	-0.012
12.099	7.3089	23.4	$K_2W_3O_{10}$	7.3200	70.0	-1 0 2	12.081	-0.018
16.189	5.4706	1.8	$K_2W_3O_{10}$	5.4500	10.0	-2 0 1	16.250	0.062
16.968	5.2209	6.1	$K_2W_3O_{10}$	5.2200	20.0	-1 0 3	16.971	0.003
17.479	5.0696	17.0	$K_2W_3O_{10}$	5.0600	40.0		17.512	0.034
19.798	4.4806	3.9	$K_2W_3O_{10}$	4.4800	20.0	2 0 1	19.801	0.003
20.579	4.3124	2.7						
21.428	4.1433	5.2						
21.858	4.0628	36.3	$K_2W_3O_{10}$	4.0600	70.0	1 0 3	21.873	0.015
22.268	3.9889	14.8	$K_2W_3O_{10}$	3.9900	40.0	-1 0 4	22.262	-0.006
22.988	3.8656	99.3	$K_2W_3O_{10}$	3.8600	80.0	0 1 0	23.022	0.034
23.638	3.7608	9.7	$K_2W_3O_{10}$	3.7600	20.0	0 0 4	23.643	0.005
24.578	3.6190	25.8	$K_2W_3O_{10}$	3.6100	60.0	-1 1 1	24.640	0.063
26.018	3.4219	44.1	$K_2W_3O_{10}$	3.4100	60.0	-1 1 2	26.110	0.093
27.227	3.2726	6.0	$K_2W_3O_{10}$	3.2700	40.0	1 0 4	27.249	0.022
28.187	3.1633	95.4	$K_2W_3O_{10}$	3.1600	100.0	-2 1 1	28.217	0.030
28.907	3.0861	100.0	$K_2W_3O_{10}$	3.0800	100.0	-3 0 4	28.966	0.059
29.417	3.0338	73.1	$K_2W_3O_{10}$	3.0300	80.0	0 0 5	29.454	0.037
30.047	2.9716	11.2	$K_2W_3O_{10}$	2.9700	20.0		30.063	0.016
31.897	2.8033	38.8	$K_2W_3O_{10}$	2.8000	70.0	3 0 2	31.936	0.039
33.137	2.7012	20.4	$K_2W_3O_{10}$	2.7000	60.0	0 1 4	33.152	0.015
33.807	2.6492	25.2	$K_2W_3O_{10}$	2.6300	60.0	-3 1 2	34.061	0.254
35.087 <sup>a</sup>	2.5555	2.0	$K_2W_3O_{10}$	2.548	-	-3 1 3	35.199	0.112
36.056	2.4889	1.0						
36.676	2.4483	29.6	$K_2W_3O_{10}$	2.4400	60.0	-3 0 6	36.805	0.129
37.216 <sup>a</sup>	2.4140	23.0	$K_2W_3O_{10}$	2.409	-	-3 1 4	37.289	0.073
37.656	2.3868	21.3	$K_2W_3O_{10}$	2.4000	60.0	-2 1 5	37.441	-0.215
38.786	2.3198	4.6	$K_2W_3O_{10}$	2.3200	20.0	2 0 5	38.783	-0.003
39.716 <sup>a</sup>	2.2676	1.1	$K_2W_3O_{10}$	2.264	-	3 1 2	39.783	0.067
40.376 <sup>a</sup>	2.2320	8.9	$K_2W_3O_{10}$	2.240	-	-3 1 5	40.218	-0.158
41.176	2.1905	12.0	$K_2W_3O_{10}$	2.1860	60.0	2 1 4	41.265	0.089
42.845	2.1089	2.5	$K_2W_3O_{10}$	2.1200	10.0	-5 0 4	42.611	-0.234
43.865	2.0622	5.5	$K_2W_3O_{10}$	2.0500	40.0	5 0 0	44.141	0.275
44.666 <sup>a</sup>	2.0271	2.6	$K_2W_3O_{10}$	2.022	-	-4 1 5	44.775	0.109
45.525	1.9908	6.5	$K_2W_3O_{10}$	1.9860	20.0	1 0 7	45.642	0.117
46.275 <sup>a</sup>	1.9603	3.0	$K_2W_3O_{10}$	1.9609	-	1 1 6	46.260	-0.015
46.935	1.9343	23.9	$K_2W_3O_{10}$	1.9280	20.0	-5 0 6	47.097	0.162
47.725	1.9041	8.2	$K_2W_3O_{10}$	1.9070	20.0	-4 1 6	47.647	-0.078
48.295 <sup>a</sup>	1.8829	6.3	$K_2W_3O_{10}$	1.8851	-	0 0 8	48.235	-0.060
50.045	1.8211	17.9	$K_2W_3O_{10}$	1.8300	20.0	-4 0 8	49.785	-0.259

<sup>a</sup> Reflections were indexed manually by calculating  $d$ -spacings and  $2\theta$ -angles for monoclinic cell of  $K_2W_3O_{10}$ .

Table S2

Phase identification for a sample of  $K_9[(ReO)_3(AsW_9O_{33})_2] \cdot n H_2O$  heated to 725 °C in DSC apparatus under N<sub>2</sub> atmosphere

$2\theta$ (obs)	$d$ (obs) (Å)	$I$ (obs) (%)	Phase ID	$d$ (card) (Å)	$I$ (card) (%)	$h$	$k$	$l$	$2\theta$ (card)	$\Delta(2\theta)$
11.809	7.4878	1.6	$K_2W_3O_{10}$	7.5400	70.0	0	0	2	11.727	-0.082
12.199	7.2493	5.2	$K_2W_3O_{10}$	7.3200	70.0	-1	0	2	12.081	-0.118
14.019	6.3120	3.9								
16.349	5.4172	1.9	$K_2W_3O_{10}$	5.4500	10.0	-2	0	1	16.250	-0.099
17.009	5.2086	2.3	$K_2W_3O_{10}$	5.2200	20.0	-1	0	3	16.971	-0.037
17.508	5.0612	7.5	$K_2W_3O_{10}$	5.0600	40.0				17.512	0.004
19.829	4.4738	3.0	$K_2W_3O_{10}$	4.4800	20.0	2	0	1	19.801	-0.028
21.538	4.1225	18.1								
21.948	4.0463	26.4	$K_2W_3O_{10}$	4.0600	70.0	1	0	3	21.873	-0.075
22.358	3.9730	12.7	$K_2W_3O_{10}$	3.9900	40.0	-1	0	4	22.262	-0.096
23.078	3.8508	55.1	$K_2W_3O_{10}$	3.8600	80.0	0	1	0	23.022	-0.056
23.757	3.7421	8.3	$K_2W_3O_{10}$	3.7600	20.0	0	0	4	23.643	-0.114
24.668	3.6060	17.9	$K_2W_3O_{10}$	3.6100	60.0	-1	1	1	24.640	-0.027
26.118	3.4091	30.1	$K_2W_3O_{10}$	3.4100	60.0	-1	1	2	26.110	-0.007
27.317	3.2620	7.4	$K_2W_3O_{10}$	3.2700	40.0	1	0	4	27.249	-0.068
28.277	3.1534	100.0	$K_2W_3O_{10}$	3.1600	100.0	-2	1	1	28.217	-0.060
29.007	3.0757	76.3	$K_2W_3O_{10}$	3.0800	100.0	-3	0	4	28.966	-0.041
29.557	3.0197	56.1	$K_2W_3O_{10}$	3.0300	80.0	0	0	5	29.454	-0.103
30.177	2.9591	13.5	$K_2W_3O_{10}$	2.9700	20.0				30.063	-0.113
30.566 <sup>a</sup>	2.9223	2.2	$K_2W_3O_{10}$	2.914	-	2	1	1	30.657	0.091
32.017	2.7931	32.1	$K_2W_3O_{10}$	2.8000	70.0	3	0	2	31.936	-0.081
33.247	2.6925	17.7	$K_2W_3O_{10}$	2.7000	60.0	0	1	4	33.152	-0.094
33.947	2.6386	19.6	$K_2W_3O_{10}$	2.6300	60.0	-3	1	2	34.061	0.115
34.926 <sup>a</sup>	2.5668	1.7	$K_2W_3O_{10}$	2.569	-	4	0	0	34.889	-0.037
35.276 <sup>a</sup>	2.5422	1.8	$K_2W_3O_{10}$	2.543	-	-4	0	4	35.260	-0.016
36.196 <sup>a</sup>	2.4796	1.3	$K_2W_3O_{10}$	2.480	-	3	0	3	36.189	-0.007
36.806	2.4399	33.5	$K_2W_3O_{10}$	2.4400	60.0	-3	0	6	36.805	-0.001
37.346	2.4059	22.3	$K_2W_3O_{10}$	2.4000	60.0	-2	1	5	37.441	0.095
37.796	2.3782	18.5	$K_2W_3O_{10}$	2.3700	60.0	-4	0	5	37.933	0.137
38.906	2.3129	4.8	$K_2W_3O_{10}$	2.3200	20.0	2	0	5	38.783	-0.124
39.736 <sup>a</sup>	2.2665	1.8	$K_2W_3O_{10}$	2.267	-	-2	0	7	39.718	-0.018
40.756 <sup>a</sup>	2.2121	7.6	$K_2W_3O_{10}$	2.221, 2.203	-	4	0	2, 4	40.575, 40.923	-0.177, 0.167
41.316	2.1834	13.9	$K_2W_3O_{10}$	2.1860	60.0	2	1	4	41.265	-0.051
42.556	2.1226	2.5	$K_2W_3O_{10}$	2.1200	10.0	-5	0	4	42.611	0.055
43.015 <sup>a</sup>	2.1010	3.4	$K_2W_3O_{10}$	2.106	-	0	1	6	42.902	-0.113
44.035	2.0547	7.1	$K_2W_3O_{10}$	2.0500	40.0	5	0	0	44.141	0.105
44.786 <sup>a</sup>	2.0220	4.6	$K_2W_3O_{10}$	2.022	-	-4	1	5	44.775	-0.011
45.355	1.9979	3.9	$K_2W_3O_{10}$	1.9960	40.0	-2	0	8	45.401	0.045
45.705	1.9834	6.9	$K_2W_3O_{10}$	1.9860	20.0	1	0	7	45.642	-0.063
46.475 <sup>a</sup>	1.9523	5.8	$K_2W_3O_{10}$	1.951	-	-1	1	7	46.500	0.025
47.155	1.9258	53.9	$K_2W_3O_{10}$	1.9280	20.0	-5	0	6	47.097	-0.058
47.855	1.8992	10.5	$K_2W_3O_{10}$	1.9070	20.0	-4	1	6	47.647	-0.208
48.465	1.8767	7.4	$K_2W_3O_{10}$	1.8700	20.0	2	2	2	48.650	0.186
49.565	1.8376	4.7	$K_2W_3O_{10}$	1.8300	20.0	-4	0	8	49.785	0.220

<sup>a</sup> Reflections were indexed manually by calculating  $d$ -spacings and  $2\theta$ -angles for monoclinic cell of  $K_2W_3O_{10}$ .

Table S3

Phase identification for a sample of  $K_9[(ReO)_3(AsW_9O_{33})_2] \cdot n H_2O$  heated to 900 °C in TGA apparatus under nitrogen atmosphere

$2\theta$ (obs)	$d$ (obs) (Å)	$I$ (obs) (%)	Phase ID	$d$ (card) (Å)	$I$ (card) (%)	$h k l$	$2\theta$ (card)	$\Delta(2\theta)$
14.089	6.2810	3.4						
15.079	5.8707	100.0	$KCr_{0.33}W_{1.67}O_6$	5.8800	100.0	1 1 1	15.055	-0.024
21.498	4.1300	8.1						
23.858	3.7266	4.9						
27.687	3.2193	2.1						
28.317	3.1490	5.6	Si	3.13549		1 1 1	28.4423	0.1253
28.937	3.0830	24.4	$KCr_{0.33}W_{1.67}O_6$	3.0700	100.0	3 1 1	29.062	0.125
30.307	2.9467	13.2	$KCr_{0.33}W_{1.67}O_6$	2.9400	85.0	2 2 2	30.378	0.070
34.346	2.6088	1.6						
35.246	2.5442	2.2	$KCr_{0.33}W_{1.67}O_6$	2.5460	15.0	4 0 0	35.221	-0.025
37.306	2.4083	2.5						
38.486	2.3372	1.6	$KCr_{0.33}W_{1.67}O_6$	2.3370	15.0	3 3 1	38.489	0.003
46.255	1.9611	1.8	$KCr_{0.33}W_{1.67}O_6$	1.9600	35.0	5 1 1	46.283	0.027
47.235	1.9227	8.9	Si	1.9201		2 2 0	47.3027	0.068
48.035	1.8925	26.3						
50.635	1.8013	3.9	$KCr_{0.33}W_{1.67}O_6$	1.8000	50.0	4 4 0	50.673	0.038
53.185	1.7208	3.1	$KCr_{0.33}W_{1.67}O_6$	1.7220	30.0	5 3 1	53.143	-0.041
56.314	1.6323	1.8	Si	1.63745		3 1 1	56.1222	-0.192
57.084	1.6121	1.5						
59.513	1.5520	2.3	$KCr_{0.33}W_{1.67}O_6$	1.5550	15.0	5 3 3	59.387	-0.127
60.332	1.5329	3.8	$KCr_{0.33}W_{1.67}O_6$	1.5370	40.0	6 2 2	60.153	-0.179
63.174	1.4706	0.7	$KCr_{0.33}W_{1.67}O_6$	1.4720	10.0	4 4 4	63.106	-0.067
63.523	1.4633	1.4						
65.373	1.4263	2.9	$KCr_{0.33}W_{1.67}O_6$	1.4290	20.0	7 1 1	65.236	-0.137
71.052	1.3256	2.0	$KCr_{0.33}W_{1.67}O_6$	1.3290	25.0	7 3 1	70.844	-0.208
71.372	1.3205	1.0						
74.762	1.2688	3.4						
81.611	1.1787	0.9	$KCr_{0.33}W_{1.67}O_6$	1.1780	5.0	7 5 1	81.671	0.060
82.581	1.1673	2.1	$KCr_{0.33}W_{1.67}O_6$	1.1700	20.0	6 6 2	82.350	-0.231
84.931	1.1409	0.6	$KCr_{0.33}W_{1.67}O_6$	1.1400	15.0	8 4 0	85.015	0.084

Table S4

Phase identification for a sample of  $(\text{NH}_4)_9[(\text{ReO})_3(\text{AsW}_9\text{O}_{33})_2] \cdot n \text{ H}_2\text{O}$  heated to 600 °C in TGA apparatus under  $\text{N}_2$  atmosphere

$2\theta(\text{obs})$	$d(\text{obs}) (\text{\AA})$	$I(\text{obs}) (\%)$	Phase ID	$d(\text{card}) (\text{\AA})$	$I(\text{card}) (\%)$	$h \ k \ l$	$2\theta(\text{card})$	$\Delta(2\theta)$
14.009	6.3165	5.2	hexagonal <sup>a</sup>	6.3264	53.0	1 0 0	13.987	-0.022
21.518	4.1263	2.5						
22.938	3.8739	84.5	tetragonal <sup>b</sup>	3.8600	70.0	0 0 1	23.022	0.084
23.938	3.7143	100.0	tetragonal	3.7100	100.0	1 1 0	23.966	0.028
26.278	3.3887	2.4						
26.677	3.3388	3.4						
28.077	3.1754	42.6	hexagonal	3.1642	100.0	2 0 0	28.179	0.102
28.637	3.1146	24.3	tetragonal	3.1100	30.0	1 0 1	28.680	0.043
33.397	2.6808	64.1	tetragonal	2.6730	60.0	1 1 1	33.497	0.100
34.107	2.6266	38.7	hexagonal	2.6245	14.0	1 1 2	34.135	0.028
35.587	2.5207	1.3						
36.896	2.4342	19.4	hexagonal	2.4244	42.0	2 0 2	37.051	0.155
41.486	2.1749	19.6	tetragonal	2.1700	25.0	2 0 1	41.583	0.097
45.085	2.0092	9.0	tetragonal	2.0050	12.0	2 1 1	45.186	0.100
46.835	1.9382	7.9	tetragonal	1.9290	8.0	0 0 2	47.071	0.236
47.964	1.8951	0.9	hexagonal	1.8859	9.0	0 0 4	48.213	0.249
48.975	1.8584	12.2	tetragonal	1.8540	16.0	2 2 0	49.098	0.123
49.685	1.8335	8.4	hexagonal	1.8269	33.0	2 2 0	49.875	0.190
50.095	1.8194	19.3	tetragonal	1.811	33.0	1 0 2	50.344	0.249
51.855	1.7617	1.2	hexagonal	1.7553	6.0	3 1 0	52.058	0.203
53.264	1.7184	12.2	tetragonal	1.7130	12.0	1 1 2	53.445	0.180
55.094	1.6656	17.7	tetragonal	1.6720	14.0	2 2 1	54.864	-0.230
56.474	1.6281	5.4	hexagonal	1.6206	15.0	2 0 4	56.760	0.286
57.994	1.5890	3.8	hexagonal	1.5915	8.0	3 1 2	57.894	-0.100
59.224	1.5589	3.4	tetragonal	1.5550	8.0	2 0 2	59.387	0.163
60.673	1.5251	9.5	tetragonal	1.5240	20.0	3 1 1	60.720	0.047
62.083	1.4938	8.5	tetragonal	1.4910	14.0	2 1 2	62.212	0.128

<sup>a</sup> Hexagonal diffraction pattern is compared with the diffraction pattern of hexagonal  $\text{KAl}_{0.33}\text{W}_{2.67}\text{O}_9$  ( $a = 7.307 \text{ \AA}$ ,  $c = 7.546 \text{ \AA}$ ).<sup>b</sup> Tetragonal diffraction pattern is compared with a diffraction pattern of tetragonal  $\text{Ca}_{0.035}\text{WO}_3$  ( $a = 5.246 \text{ \AA}$ ,  $c = 3.858 \text{ \AA}$ ).

Table S5

Phase identification for a sample of  $(\text{NH}_4)_9[(\text{ReO})_3(\text{AsW}_9\text{O}_{33})_2] \cdot n \text{ H}_2\text{O}$  heated to 725 °C in DSC apparatus under N<sub>2</sub> atmosphere

$2\theta(\text{obs})$	$d(\text{obs}) (\text{\AA})$	$I(\text{obs}) (\%)$	Phase ID	$d(\text{card}) (\text{\AA})$	$I(\text{card}) (\%)$	$h \ k \ l$	$2\theta(\text{card})$	$\Delta(2\theta)$
14.039	6.3031	4.3	hexagonal <sup>a</sup>	6.3264	53.0	1 0 0	13.987	-0.052
19.368	4.5791	1.5						
21.498	4.1300	3.9						
22.938	3.8739	60.9	tetragonal <sup>b</sup>	3.8600	70.0	0 0 1	23.022	0.084
23.528	3.7781	16.9	hexagonal	3.7730	33.0	0 0 2	23.560	0.032
23.978	3.7082	100.0	tetragonal	3.7100	100.0	1 1 0	23.966	-0.012
26.818	3.3217	2.7						
28.107	3.1721	33.2	hexagonal	3.1642	100.0	2 0 0	28.179	0.072
28.617	3.1167	20.7	tetragonal	3.1100	30.0	1 0 1	28.680	0.063
33.407	2.6800	55.1	tetragonal	2.6730	60.0	1 1 1	33.497	0.090
34.147	2.6236	31.7	tetragonal	2.6240	45.0	2 0 0	34.141	-0.005
35.526	2.5248	1.5						
35.646	2.5166	1.3						
36.926	2.4323	16.5	hexagonal	2.4244	42.0	2 0 2	37.051	0.125
41.516	2.1734	18.6	tetragonal	2.1700	25.0	2 0 1	41.583	0.067
45.115	2.0080	9.0	tetragonal	2.0050	12.0	2 1 1	45.186	0.070
46.855	1.9374	6.5	tetragonal	1.9290	8.0	0 0 2	47.071	0.216
47.965	1.8951	1.5	hexagonal	1.8859	9.0	0 0 4	48.213	0.248
49.035	1.8562	12.0	tetragonal	1.8540	16.0	2 2 0	49.098	0.063
49.655	1.8345	5.1	hexagonal	1.8413	6.0	3 0 2	49.460	-0.195
50.085	1.8198	13.7	hexagonal	1.8269	33.0	2 2 0	49.875	-0.210
50.314	1.8120	9.7	tetragonal	1.8110	20.0	1 0 2	50.344	0.030
51.944	1.7589	1.1	hexagonal	1.7553	6.0	3 1 0	52.058	0.114
53.294	1.7175	9.3	tetragonal	1.7130	12.0	1 1 2	53.445	0.150
53.504	1.7113	5.9	hexagonal	1.7099	1.0	3 1 1	53.550	0.046
54.874	1.6717	13.3	tetragonal	1.6720	14.0	2 2 1	54.864	-0.011
55.304	1.6597	15.4	tetragonal	1.6590	20.0	3 1 0	55.330	0.026
56.634	1.6239	3.3	hexagonal	1.6206	15.0	2 0 4	56.760	0.126
57.944	1.5902	3.0	hexagonal	1.5915	8.0	3 1 2	57.894	-0.050
58.164	1.5848	2.8	hexagonal	1.5823	15.0	4 0 0	58.264	0.100
59.094	1.5620	3.5	tetragonal	1.5550	8.0	2 0 2	59.387	0.293
60.693	1.5246	12.1	tetragonal	1.5240	20.0	3 1 1	60.720	0.027

<sup>a</sup> Hexagonal diffraction pattern is compared with the diffraction pattern of hexagonal KAl<sub>0.33</sub>W<sub>2.67</sub>O<sub>9</sub> ( $a = 7.307 \text{ \AA}$ ,  $c = 7.546 \text{ \AA}$ ).<sup>b</sup> Tetragonal diffraction pattern is compared with a diffraction pattern of tetragonal Ca<sub>0.035</sub>WO<sub>3</sub> ( $a = 5.246 \text{ \AA}$ ,  $c = 3.858 \text{ \AA}$ ).

Table S6

Phase identification for a sample of  $(\text{NH}_4)_9[(\text{ReO})_3(\text{AsW}_9\text{O}_{33})_2] \cdot n \text{ H}_2\text{O}$  heated to 900 °C in TGA apparatus under  $\text{N}_2$  atmosphere

$2\theta(\text{obs})$	$d(\text{obs}) (\text{\AA})$	$I(\text{obs}) (\%)$	Phase ID	$d(\text{card}) (\text{\AA})$	$I(\text{card}) (\%)$	$h \ k \ l$	$2\theta(\text{card})$	$\Delta(2\theta)$
14.019	6.3122	3.2	hexagonal <sup>a</sup>	6.3264	53.0	1 0 0	13.987	-0.032
19.329	4.5884	1.6						
21.508	4.1282	1.1						
23.088	3.8492	37.9	orthorhombic <sup>b</sup>	3.8500	100.0	0 0 1	23.082	-0.005
23.568	3.7718	100.0	hexagonal	3.7730	33.0	0 0 2	23.560	-0.008
23.747	3.7437	37.9	orthorhombic	3.7500	65.0	0 2 0	23.707	-0.040
24.208	3.6735	74.4	orthorhombic	3.6900	95.0	2 0 0	24.098	-0.110
26.027	3.4207	0.5	orthorhombic	3.4300	2.0	0 1 1	25.955	-0.072
26.687	3.3376	5.4	orthorhombic	3.3500	10.0	1 2 0	26.586	-0.101
27.527	3.2376	2.0	hexagonal	3.2408	20.0	1 0 2	27.500	-0.027
28.227	3.1589	18.6	hexagonal	3.1642	100.0	2 0 0	28.179	-0.048
28.687	3.1093	26.6	orthorhombic	3.1000	25.0	1 1 1	28.775	0.088
33.267	2.6909	66.2	orthorhombic	2.6860	35.0	0 2 1	33.330	0.063
33.637	2.6622	35.4	orthorhombic	2.6620	35.0	2 0 1	33.639	0.003
34.167	2.6221	38.5	hexagonal	2.6245	14.0	1 1 2	34.135	-0.032
35.586	2.5207	7.5	orthorhombic	2.5250	6.0	1 2 1	35.524	-0.063
36.126	2.4843	1.5						
37.196	2.4152	23.8	hexagonal	2.4244	42.0	2 0 2	37.051	-0.145
41.586	2.1699	21.7	orthorhombic	2.1730	16.0	2 2 1	41.523	-0.063
42.945	2.1043	1.4	hexagonal	2.1095	5.0	3 0 0	42.834	-0.111
44.135	2.0502	2.9	orthorhombic	2.0560	2.0	3 2 0	44.005	-0.130
44.355	2.0406	1.4						
44.885	2.0177	4.7	orthorhombic	2.0180	10.0	1 3 1	44.879	-0.007
45.465	1.9933	6.8	orthorhombic	1.9980	6.0	3 1 1	45.353	-0.112
45.815	1.9789	2.5						
47.035	1.9304	8.7	orthorhombic	1.9230	20.0	0 0 2	47.227	0.191
48.585	1.8724	6.2	orthorhombic	1.8780	10.0	0 4 0	48.430	-0.155
48.814	1.8641	1.7	orthorhombic	1.863	-	0 1 2	48.847	0.033
49.480	1.8406	4.7	hexagonal	1.8413	6.0	3 0 2	49.460	-0.020
49.805	1.8293	10.0	hexagonal	1.8269	33.0	2 2 0	49.875	0.070
50.355	1.8106	24.0	hexagonal	1.8079	2.0	1 0 4	50.436	0.081
52.134	1.7529	1.3	hexagonal	1.7553	6.0	3 1 0	52.058	-0.076
53.554	1.7098	5.6	hexagonal	1.7099	1.0	3 1 1	53.550	-0.004
53.794	1.7027	5.6	orthorhombic	1.7060	10.0	2 0 2	53.682	-0.113
54.334	1.6870	7.3	orthorhombic	1.6880	16.0	0 4 1	54.301	-0.033
54.555	1.6807	9.8	hexagonal	1.6765	2.0	1 1 4	54.704	0.150
54.964	1.6692	4.9	orthorhombic	1.6650	16.0	4 0 1	55.114	0.150
55.434	1.6561	9.4	orthorhombic	1.6570	16.0	4 2 0	55.403	-0.031
55.774	1.6468	12.4	orthorhombic	1.6450	6.0	1 4 1	55.842	0.068
56.664	1.6231	4.6	hexagonal	1.6206	15.0	2 0 4	56.760	0.096
56.954	1.6155	3.3						
57.864	1.5922	4.1	hexagonal	1.5915	8.0	3 1 2	57.894	0.030
58.184	1.5842	2.1	hexagonal	1.5823	15.0	4 0 0	58.264	0.080

<sup>a</sup> Hexagonal diffraction pattern is compared with the diffraction pattern of hexagonal  $\text{KAl}_{0.33}\text{W}_{2.67}\text{O}_9$  ( $a = 7.307 \text{ \AA}$ ,  $c = 7.546 \text{ \AA}$ ).<sup>b</sup> Orthorhombic diffraction pattern is compared with the diffraction pattern of orthorhombic  $\text{WO}_3$  ( $a = 7.384 \text{ \AA}$ ,  $b = 7.512 \text{ \AA}$ ,  $c = 3.846 \text{ \AA}$ ).

Table S7

Unit cell refinement results of a sample of  $K_9[(ReO_3)(AsW_9O_{33})_2] \cdot n H_2O$  heated to 600 °C in TGA apparatus under  $N_2$  atmosphere

<i>h</i>	<i>k</i>	<i>l</i>	2θ(cal)	2θ(obs)	Δ(2θ)	<i>d</i> (cal) (Å)	<i>d</i> (obs) (Å)	Δ( <i>d</i> ) (Å)
0	0	2	11.712	11.739	-0.027	7.5496	7.5323	0.0173
-1	0	2	12.057	12.099	-0.042	7.3344	7.3089	0.0255
-2	0	1	16.236	16.189	0.048	5.4547	5.4706	-0.0159
-1	0	3	16.889	16.968	-0.079	5.2452	5.2209	0.0243
-2	0	2	17.368	17.479	-0.111	5.1018	5.0696	0.0321
2	0	1	19.897	19.798	0.099	4.4586	4.4806	-0.0220
1	0	3	22.005	21.858	0.147	4.0360	4.0628	-0.0268
-1	0	4	22.273	22.268	0.005	3.9880	3.9889	-0.0009
0	1	0	22.896	22.988	-0.092	3.8809	3.8656	0.0153
0	0	4	23.549	23.638	-0.089	3.7748	3.7608	0.0140
-1	1	1	24.520	24.578	-0.057	3.6274	3.6190	0.0083
-1	1	2	25.953	26.018	-0.064	3.4303	3.4219	0.0083
-2	1	1	28.197	28.187	0.010	3.1622	3.1633	-0.0011
-3	0	4	28.855	28.907	-0.052	3.0916	3.0861	0.0055
0	0	5	29.556	29.417	0.139	3.0198	3.0338	-0.0139
3	0	2	31.881	31.897	-0.016	2.8047	2.8033	0.0014
0	1	4	33.078	33.137	-0.059	2.7059	2.7012	0.0047
-3	1	2	33.922	33.807	0.116	2.6405	2.6492	-0.0088
-3	0	6	36.730	36.676	0.054	2.4448	2.4483	-0.0035
-2	1	5	37.247	37.216	0.031	2.4120	2.4140	-0.0019
-4	0	5	37.758	37.656	0.102	2.3805	2.3868	-0.0062
2	1	4	41.086	41.176	-0.090	2.1951	2.1905	0.0046
5	0	0	43.834	43.865	-0.031	2.0636	2.0622	0.0014
-2	0	8	45.449	45.525	-0.077	1.9940	1.9908	0.0032
-5	0	6	46.956	46.935	0.021	1.9335	1.9343	-0.0008
-4	1	6	47.595	47.725	-0.130	1.9090	1.9041	0.0049
0	2	2	48.392	48.295	0.097	1.8794	1.8829	-0.0036

Refined cell:  $a = 10.91(2)$ ,  $b = 3.881(4)$ ,  $c = 15.97(2)$ ,  $\beta = 109.0(1)$ ,  $V = 639.4 \text{ \AA}^3$ . Agreement:  $|\Delta(2\theta)| = 0.07^\circ$ ,  $|\Delta(d)| = 0.01 \text{ \AA}$ , ESD of fit = 0.08° (ESD, estimated standard deviation).

Table S8

Unit cell refinement results for a sample of  $K_9[(ReO_3)(AsW_9O_{33})_2] \cdot n H_2O$  heated to 725 °C in DSC apparatus under N<sub>2</sub> atmosphere

<i>h k l</i>	2θ(cal)	2θ(obs)	Δ(2θ)	d(cal) (Å)	d(obs) (Å)	Δ(d)
0 0 2	11.721	11.809	-0.089	7.5441	7.4878	0.0563
-1 0 2	12.072	12.199	-0.127	7.3250	7.2493	0.0757
-2 0 1	16.310	16.349	-0.040	5.4302	5.4172	0.0131
-1 0 3	16.900	17.009	-0.109	5.2420	5.2086	0.0334
-2 0 2	17.425	17.508	-0.083	5.0851	5.0612	0.0239
2 0 1	19.985	19.829	0.157	4.4391	4.4738	-0.0348
1 0 3	22.051	21.948	0.103	4.0277	4.0463	-0.0187
-1 0 4	22.283	22.358	-0.075	3.9863	3.9730	0.0132
0 1 0	22.983	23.078	-0.094	3.8664	3.8508	0.0156
0 0 4	23.566	23.757	-0.191	3.7721	3.7421	0.0299
-1 1 1	24.613	24.668	-0.055	3.6140	3.6060	0.0080
-1 1 2	26.038	26.118	-0.079	3.4193	3.4091	0.0102
-2 1 1	28.312	28.277	0.035	3.1496	3.1534	-0.0038
-3 0 4	28.927	29.007	-0.080	3.0841	3.0757	0.0084
0 0 5	29.578	29.557	0.021	3.0177	3.0197	-0.0021
3 0 2	32.017	32.017	0.000	2.7931	2.7931	0.0000
0 1 4	33.153	33.247	-0.094	2.7000	2.6925	0.0074
-3 1 2	34.061	33.947	0.114	2.6300	2.6386	-0.0086
-3 0 6	36.779	36.806	-0.028	2.4417	2.4399	0.0018
-2 1 5	37.323	37.346	-0.023	2.4073	2.4059	0.0014
-4 0 5	37.861	37.796	0.065	2.3743	2.3782	-0.0039
2 1 4	41.215	41.316	-0.101	2.1885	2.1834	0.0051
-5 0 4	42.683	42.556	0.127	2.1166	2.1226	-0.0060
5 0 0	44.058	44.035	0.023	2.0536	2.0547	-0.0010
-2 0 8	45.469	45.355	0.114	1.9931	1.9979	-0.0048
1 0 7	45.704	45.705	-0.001	1.9835	1.9834	0.0001
-5 0 6	47.093	47.155	-0.062	1.9281	1.9258	0.0024
-4 1 6	47.720	47.855	-0.135	1.9043	1.8992	0.0051
0 2 2	48.576	48.465	0.112	1.8727	1.8767	-0.0040
-4 0 8	49.749	49.565	0.184	1.8313	1.8376	-0.0064

Refined cell:  $a = 10.86(2)$  Å,  $b = 3.866(5)$  Å,  $c = 15.96(2)$  Å,  $\beta = 109.0(1)$ . Agreement:  $|\Delta(2\theta)| = 0.08^\circ$ ,  $|\Delta(d)| = 0.014$  Å, ESD of fit = 0.1° (ESD, estimated standard deviation).

Table S9

Unit cell refinement results for a sample of  $K_9[(ReO)_3(AsW_9O_{33})_2] \cdot n H_2O$  heated to 900 °C in TGA apparatus under N<sub>2</sub> atmosphere

<i>h k l</i>	2θ(cal)	2θ(obs)	Δ(2θ)	d(cal) (Å)	d(obs) (Å)	Δ(d) (Å)
1 1 1	15.073	15.079	-0.006	5.8730	5.8707	0.0022
3 1 1	29.091	28.937	0.154	3.0671	3.0830	-0.0160
2 2 2	30.415	30.307	0.108	2.9365	2.9467	-0.0102
4 0 0	35.263	35.246	0.017	2.5431	2.5442	-0.0012
3 3 1	38.546	38.486	0.060	2.3337	2.3372	-0.0035
5 1 1	46.341	46.255	0.086	1.9577	1.9611	-0.0034
4 4 0	50.727	50.635	0.092	1.7982	1.8013	-0.0031
5 3 1	53.229	53.185	0.045	1.7194	1.7208	-0.0013
5 3 3	59.544	59.513	0.031	1.5513	1.5520	-0.0007
6 2 2	60.304	60.332	-0.028	1.5335	1.5329	0.0006
4 4 4	63.286	63.174	0.113	1.4682	1.4706	-0.0024
7 1 1	65.473	65.373	0.100	1.4244	1.4263	-0.0019
7 3 1	71.133	71.052	0.080	1.3243	1.3256	-0.0013
8 0 0	74.571	74.762	-0.190	1.2715	1.2688	0.0028
7 5 1	81.959	82.082	-0.123	1.1746	1.1731	0.0014
6 6 2	82.622	82.581	0.041	1.1668	1.1673	-0.0005
8 4 0	85.265	85.350	-0.085	1.1373	1.1364	0.0009

Refined cell:  $a = 10.172(3)$  Å (cubic). Agreement:  $|\Delta(2\theta)| = 0.08^\circ$ ,  $|\Delta(d)| = 0.003$  Å, ESD of fit = 0.1° (ESD, estimated standard deviation).

Table S10

Unit cell refinement results of hexagonal phase found in a sample of  $(NH_4)_9[(ReO)_3(AsW_9O_{33})_2] \cdot n H_2O$  heated to 600 °C in TGA apparatus under N<sub>2</sub> atmosphere

<i>h k l</i>	2θ(cal)	2θ(obs)	Δ(2θ)	d(cal) (Å)	d(obs) (Å)	Δ(d) (Å)
1 0 0	13.951	14.009	-0.058	6.3428	6.3165	0.0263
0 0 2	23.648	23.938	-0.290	3.7593	3.7143	0.0449
2 0 0	28.114	28.077	0.036	3.1714	3.1754	-0.0040
1 1 2	34.153	34.107	0.046	2.6231	2.6266	-0.0035
2 0 2	37.056	36.896	0.160	2.4240	2.4342	-0.0101
2 1 2	44.801	45.085	-0.284	2.0213	2.0092	0.0121
2 2 0	49.756	49.685	0.071	1.8310	1.8335	-0.0024
3 1 0	51.935	51.855	0.080	1.7592	1.7617	-0.0025
3 1 1	53.447	53.264	0.183	1.7129	1.7184	-0.0055
1 1 4	54.856	55.094	-0.238	1.6722	1.6656	0.0067
4 0 0	58.125	57.994	0.132	1.5857	1.5890	-0.0033
4 0 2	63.635	63.473	0.161	1.4610	1.4644	-0.0033
4 1 1	68.925	69.013	-0.088	1.3612	1.3597	0.0015
2 2 4	71.930	71.882	0.048	1.3116	1.3123	-0.0008
4 1 2	72.746	72.772	-0.027	1.2989	1.2985	0.0004
0 0 6	75.861	75.792	0.069	1.2531	1.2541	-0.0010
3 3 0	78.252	78.491	-0.239	1.2207	1.2175	0.0031
5 0 2	79.710	79.691	0.019	1.2020	1.2022	-0.0002
2 0 6	82.745	82.651	0.094	1.1654	1.1665	-0.0011
3 3 2	83.129	83.166	-0.037	1.1610	1.1606	0.0004

Refined cell:  $a = 7.324(7)$  Å,  $c = 7.519(7)$  Å,  $V = 349.3$  Å<sup>3</sup>. Agreement:  $|\Delta(2\theta)| = 0.12^\circ$ ,  $|\Delta(d)| = 0.007$  Å, ESD of fit = 0.15° (ESD, estimated standard deviation).

Table S11

Unit cell refinement results of tetragonal phase found in a sample of  $(\text{NH}_4)_9[(\text{ReO})_3(\text{AsW}_9\text{O}_{33})_2]\cdot n \text{ H}_2\text{O}$  heated to 600 °C in TGA apparatus under  $\text{N}_2$  atmosphere

$h \ k \ l$	$2\theta(\text{cal})$	$2\theta(\text{obs})$	$\Delta(2\theta)$	$d(\text{cal}) (\text{\AA})$	$d(\text{obs}) (\text{\AA})$	$\Delta(d) (\text{\AA})$
0 0 1	22.908	22.938	-0.030	3.8789	3.8739	0.0050
1 1 0	23.982	23.938	0.044	3.7076	3.7143	-0.0067
1 0 1	28.602	28.637	-0.035	3.1184	3.1146	0.0038
1 1 1	33.404	33.397	0.008	2.6802	2.6808	-0.0006
2 0 0	34.172	34.107	0.066	2.6217	2.6266	-0.0049
2 0 1	41.541	41.486	0.055	2.1721	2.1749	-0.0028
1 2 1	45.145	45.085	0.059	2.0067	2.0092	-0.0025
0 0 2	46.802	46.835	-0.033	1.9394	1.9382	0.0013
2 2 0	49.103	48.975	0.128	1.8538	1.8584	-0.0045
1 0 2	50.107	50.095	0.012	1.8190	1.8194	-0.0004
1 1 2	53.259	53.264	-0.005	1.7185	1.7184	0.0002
2 2 1	54.842	55.094	-0.252	1.6726	1.6656	0.0071
3 0 1	57.814	57.994	-0.180	1.5935	1.5890	0.0045
2 0 2	59.211	59.224	-0.012	1.5592	1.5589	0.0003
1 3 1	60.692	60.673	0.018	1.5246	1.5251	-0.0004
1 2 2	62.049	62.083	-0.034	1.4945	1.4938	0.0007
2 3 1	68.898	69.013	-0.114	1.3617	1.3597	0.0020
2 2 2	70.170	70.053	0.118	1.3401	1.3421	-0.0020
4 0 0	71.976	71.882	0.094	1.3108	1.3123	-0.0015
3 0 2	72.779	72.772	0.007	1.2984	1.2985	-0.0001
1 0 3	75.700	75.792	-0.092	1.2554	1.2541	0.0013
4 0 1	76.671	76.786	-0.115	1.2419	1.2403	0.0016
1 1 3	78.238	78.491	-0.253	1.2209	1.2175	0.0033
3 3 1	81.708	81.801	-0.093	1.1776	1.1765	0.0011
4 2 0	82.140	82.161	-0.021	1.1725	1.1722	0.0003
2 3 2	82.911	82.651	0.260	1.1635	1.1665	-0.0030
2 0 3	83.251	83.166	0.085	1.1596	1.1606	-0.0010
2 1 3	85.736	85.701	0.035	1.1322	1.1326	-0.0004

Refined cell:  $a = 5.243(2) \text{ \AA}$ ,  $c = 3.879(1) \text{ \AA}$ ,  $V = 106.6 \text{ \AA}^3$ . Agreement:  $|\Delta(2\theta)| = 0.05^\circ$ ,  $|\Delta(d)| = 0.002 \text{ \AA}$ , ESD of fit =  $0.07^\circ$  (ESD, estimated standard deviation).

Table S12

Unit cell refinement results of hexagonal phase found in a sample of  $(\text{NH}_4)_9[(\text{ReO})_3(\text{AsW}_9\text{O}_{33})_2]\cdot n \text{ H}_2\text{O}$  heated to 725 °C in DSC apparatus under  $\text{N}_2$  atmosphere

$h \ k \ l$	2θ(cal)	2θ(obs)	$\Delta(2\theta)$	d(cal) (Å)	d(obs) (Å)	$\Delta(d)$ (Å)
1 0 0	14.018	14.039	-0.021	6.3125	6.3031	0.0094
0 0 2	23.502	23.528	-0.026	3.7822	3.7781	0.0041
1 1 1	27.137	26.947	0.190	3.2833	3.3060	-0.0227
1 1 2	34.136	34.147	-0.010	2.6244	2.6236	0.0008
2 0 2	37.068	36.926	0.141	2.4233	2.4323	-0.0089
2 1 2	44.880	45.115	-0.235	2.0179	2.0080	0.0100
0 0 4	48.073	47.965	0.108	1.8911	1.8951	-0.0040
3 0 2	49.532	49.655	-0.123	1.8388	1.8345	0.0043
2 2 0	50.011	50.085	-0.074	1.8223	1.8198	0.0025
1 0 4	50.327	50.314	0.013	1.8116	1.8120	-0.0004
3 1 0	52.203	51.944	0.259	1.7508	1.7589	-0.0081
3 1 1	53.692	53.504	0.189	1.7057	1.7113	-0.0056
1 1 4	54.631	54.874	-0.243	1.6786	1.6717	0.0069
2 0 4	56.697	56.634	0.064	1.6222	1.6239	-0.0017
3 1 2	58.001	57.944	0.057	1.5888	1.5902	-0.0014
4 0 0	58.431	58.164	0.268	1.5781	1.5848	-0.0066
4 0 2	63.860	63.963	-0.103	1.4564	1.4543	0.0021
3 0 4	66.412	66.402	0.009	1.4065	1.4067	-0.0002
4 1 1	69.275	69.132	0.143	1.3552	1.3577	-0.0024
2 2 4	71.891	71.942	-0.051	1.3122	1.3114	0.0008
4 1 2	73.042	72.832	0.210	1.2943	1.2975	-0.0032
3 1 4	73.677	73.662	0.015	1.2847	1.2850	-0.0002
2 1 5	74.153	74.092	0.061	1.2777	1.2786	-0.0009
5 0 0	75.197	75.242	-0.046	1.2625	1.2618	0.0007
0 0 6	75.321	75.342	-0.021	1.2607	1.2604	0.0003
3 2 3	75.668	75.612	0.057	1.2558	1.2566	-0.0008
1 0 6	77.078	76.931	0.147	1.2363	1.2383	-0.0020
3 3 0	78.700	78.641	0.059	1.2148	1.2156	-0.0008
4 0 4	78.948	78.911	0.037	1.2117	1.2121	-0.0005
4 1 3	79.165	79.321	-0.156	1.2089	1.2069	0.0020
3 3 1	79.909	79.881	0.028	1.1995	1.1998	-0.0004
4 2 1	81.638	81.686	-0.048	1.1784	1.1778	0.0006
2 0 6	82.282	82.361	-0.078	1.1708	1.1699	0.0009
2 2 5	82.867	82.931	-0.064	1.1640	1.1633	0.0007
3 1 5	84.583	84.739	-0.156	1.1447	1.1430	0.0017
5 1 0	85.594	85.701	-0.107	1.1338	1.1326	0.0011
5 1 1	86.785	86.745	0.040	1.1212	1.1216	-0.0004

Refined cell:  $a = 7.2890(6)$  Å,  $c = 7.5644(6)$  Å,  $V = 348.1$  Å<sup>3</sup>. Agreement:  $|\Delta(2\theta)| = 0.08^\circ$ ,  $|\Delta(d)| = 0.003$  Å, ESD of fit = 0.10° (ESD, estimated standard deviation).

Table S13

Unit cell refinement results of tetragonal phase found in a sample of  $(\text{NH}_4)_9[(\text{ReO})_3(\text{AsW}_9\text{O}_{33})_2]\cdot n \text{ H}_2\text{O}$  heated to 725 °C in DSC apparatus under  $\text{N}_2$  atmosphere

$h \ k \ l$	2θ(cal)	2θ(obs)	$\Delta(2\theta)$	d(cal) (Å)	d(obs) (Å)	$\Delta(d)$ (Å)
0 0 1	22.973	22.938	0.035	3.8681	3.8739	-0.0059
1 1 0	23.971	23.978	-0.007	3.7093	3.7082	0.0011
1 1 1	33.442	33.407	0.036	2.6772	2.6800	-0.0028
2 0 0	34.157	34.147	0.010	2.6229	2.6236	-0.0007
2 0 1	41.566	41.516	0.050	2.1709	2.1734	-0.0025
1 2 1	45.165	45.115	0.049	2.0059	2.0080	-0.0021
0 0 2	46.941	46.855	0.086	1.9340	1.9374	-0.0034
2 2 0	49.079	49.035	0.044	1.8546	1.8562	-0.0016
1 0 2	50.236	50.314	-0.078	1.8146	1.8120	0.0026
1 1 2	53.380	53.294	0.086	1.7149	1.7175	-0.0026
2 2 1	54.851	54.874	-0.023	1.6723	1.6717	0.0006
1 3 0	55.336	55.304	0.032	1.6588	1.6597	-0.0009
3 0 1	57.820	57.944	-0.124	1.5933	1.5902	0.0031
2 0 2	59.319	59.094	0.225	1.5566	1.5620	-0.0054
1 3 1	60.695	60.693	0.002	1.5246	1.5246	0.0000
1 2 2	62.152	62.003	0.148	1.4923	1.4955	-0.0032
2 3 0	63.935	63.963	-0.029	1.4549	1.4543	0.0006
2 3 1	68.895	68.922	-0.028	1.3618	1.3613	0.0005
2 2 2	70.259	70.322	-0.063	1.3386	1.3376	0.0010
4 0 0	71.939	71.942	-0.003	1.3114	1.3114	0.0000
3 0 2	72.864	72.832	0.032	1.2971	1.2975	-0.0005
1 3 2	75.433	75.452	-0.019	1.2591	1.2589	0.0003
1 0 3	75.933	75.921	0.012	1.2521	1.2522	-0.0002
4 0 1	76.661	76.672	-0.011	1.2420	1.2418	0.0001
3 3 0	77.069	76.931	0.138	1.2364	1.2383	-0.0019
1 1 3	78.467	78.521	-0.055	1.2179	1.2172	0.0007
4 1 1	79.188	79.321	-0.133	1.2086	1.2069	0.0017
3 3 1	81.694	81.686	0.008	1.1777	1.1778	-0.0001
4 2 0	82.095	82.061	0.034	1.1730	1.1734	-0.0004
2 3 2	82.984	82.931	0.053	1.1627	1.1633	-0.0006
2 1 3	85.953	85.970	-0.017	1.1299	1.1298	0.0002

Refined cell:  $a = 5.2457(9)$  Å,  $c = 3.868(1)$  Å,  $V = 106.4$  Å<sup>3</sup>. Agreement:  $|\Delta(2\theta)| = 0.036^\circ$ ,  $|\Delta(d)| = 0.0012$  Å, ESD of fit = 0.05° (ESD, estimated standard deviation).

Table S14

Unit cell refinement results of hexagonal phase found in a sample of  $(\text{NH}_4)_9[(\text{ReO})_3(\text{AsW}_9\text{O}_{33})_2]\cdot n \text{ H}_2\text{O}$  heated to 900 °C in TGA apparatus under  $\text{N}_2$  atmosphere

t	2θ(cal)	2θ(obs)	$\Delta(2\theta)$	d(cal) (Å)	d(obs) (Å)	$\Delta(d)$ (Å)
1 0 0	13.966	14.019	-0.053	6.3359	6.3122	0.0237
0 0 2	23.560	23.568	-0.007	3.7730	3.7718	0.0011
1 1 0	24.312	24.208	0.104	3.6580	3.6735	-0.0155
1 0 2	27.491	27.527	-0.036	3.2417	3.2376	0.0041
2 0 0	28.145	28.227	-0.083	3.1680	3.1589	0.0091
1 1 2	34.110	34.167	-0.056	2.6263	2.6221	0.0042
2 0 2	37.023	37.196	-0.174	2.4261	2.4152	0.0109
3 0 0	42.781	42.945	-0.165	2.1120	2.1043	0.0077
2 1 2	44.788	44.885	-0.097	2.0219	2.0177	0.0042
3 0 2	49.413	49.480	-0.067	1.8429	1.8406	0.0023
2 2 0	49.814	49.805	0.009	1.8290	1.8293	-0.0003
1 0 4	50.432	50.355	0.077	1.8080	1.8106	-0.0026
2 2 1	51.359	51.235	0.124	1.7776	1.7816	-0.0040
3 1 0	51.996	52.134	-0.138	1.7573	1.7529	0.0043
2 1 3	52.734	52.654	0.079	1.7344	1.7368	-0.0024
3 1 1	53.496	53.554	-0.058	1.7115	1.7098	0.0017
1 1 4	54.699	54.555	0.144	1.6767	1.6807	-0.0041
2 2 2	55.812	55.774	0.037	1.6458	1.6468	-0.0010
2 0 4	56.748	56.664	0.084	1.6209	1.6231	-0.0022
3 1 2	57.835	57.864	-0.029	1.5930	1.5922	0.0007
4 0 0	58.195	58.184	0.011	1.5840	1.5842	-0.0003
2 1 4	62.636	62.483	0.153	1.4819	1.4852	-0.0033
4 0 2	63.661	63.713	-0.052	1.4605	1.4594	0.0011
3 2 0	64.001	63.993	0.008	1.4536	1.4537	-0.0002
3 0 4	66.389	66.433	-0.043	1.4069	1.4061	0.0008
1 1 5	67.026	67.123	-0.097	1.3951	1.3933	0.0018
4 1 0	67.714	67.662	0.052	1.3826	1.3835	-0.0009
3 2 2	69.207	69.413	-0.206	1.3564	1.3529	0.0035
4 1 2	72.790	72.692	0.098	1.2982	1.2997	-0.0015
3 1 4	73.604	73.482	0.122	1.2858	1.2877	-0.0018
2 1 5	74.212	73.932	0.280	1.2768	1.2809	-0.0041
0 0 6	75.537	75.682	-0.145	1.2577	1.2556	0.0020
4 1 3	78.949	79.151	-0.202	1.2116	1.2090	0.0026
3 3 1	79.570	79.631	-0.061	1.2037	1.2030	0.0008
4 2 0	80.078	80.111	-0.033	1.1974	1.1970	0.0004
1 1 6	80.731	80.591	0.139	1.1893	1.1910	-0.0017
4 2 1	81.288	81.083	0.205	1.1826	1.1851	-0.0025
2 0 6	82.443	82.481	-0.038	1.1689	1.1685	0.0004
2 2 5	82.861	83.021	-0.160	1.1641	1.1622	0.0018
3 2 4	83.978	83.911	0.067	1.1514	1.1522	-0.0007
3 1 5	84.565	84.430	0.135	1.1449	1.1464	-0.0015
4 2 2	84.897	84.930	-0.034	1.1413	1.1409	0.0004
5 1 1	86.400	86.350	0.050	1.1252	1.1258	-0.0005
2 1 6	87.545	87.560	-0.015	1.1134	1.1133	0.0002

Refined cell:  $a = 7.316(4)$  Å,  $c = 7.545(3)$  Å,  $V = 349.8$  Å<sup>3</sup>. Agreement:  $|\Delta(2\theta)| = 0.09^\circ$ ,  $|\Delta(d)| = 0.003$  Å, ESD of fit = 0.11° (ESD, estimated standard deviation).

Table S15

Unit cell refinement results of orthorhombic phase found in a sample of  $(\text{NH}_4)_9[(\text{ReO})_3(\text{AsW}_9\text{O}_{33})_2] \cdot n \text{ H}_2\text{O}$  heated to 900 °C in TGA apparatus under  $\text{N}_2$  atmosphere

$h \ k \ l$	$2\theta(\text{cal})$	$2\theta(\text{obs})$	$\Delta(2\theta)$	$d(\text{cal}) (\text{\AA})$	$d(\text{obs}) (\text{\AA})$	$\Delta(d) (\text{\AA})$
0 0 1	23.024	23.088	-0.063	3.8596	3.8492	0.0104
0 2 0	23.710	23.747	-0.037	3.7495	3.7437	0.0057
2 0 0	24.124	24.208	-0.084	3.6860	3.6735	0.0125
0 1 1	25.942	26.027	-0.085	3.4317	3.4207	0.0110
1 2 0	26.651	26.687	-0.036	3.3420	3.3376	0.0045
1 1 1	28.670	28.687	-0.018	3.1111	3.1093	0.0019
0 2 1	33.287	33.267	0.020	2.6894	2.6909	-0.0016
2 0 1	33.592	33.637	-0.045	2.6657	2.6622	0.0034
2 2 0	34.080	34.167	-0.086	2.6286	2.6221	0.0064
1 2 1	35.502	35.586	-0.084	2.5265	2.5207	0.0058
2 2 1	41.532	41.586	-0.054	2.1726	2.1699	0.0027
0 3 1	43.079	42.945	0.133	2.0981	2.1043	-0.0062
3 2 0	44.021	44.135	-0.114	2.0553	2.0502	0.0050
1 3 1	44.880	44.885	-0.005	2.0179	2.0177	0.0002
3 1 1	45.354	45.465	-0.111	1.9979	1.9933	0.0046
0 0 2	47.051	47.035	0.016	1.9298	1.9304	-0.0006
0 4 0	48.520	48.585	-0.065	1.8747	1.8724	0.0024
4 0 0	49.410	49.480	-0.070	1.8430	1.8406	0.0025
1 1 2	50.326	50.355	-0.028	1.8116	1.8106	0.0010
2 0 2	53.558	53.554	0.003	1.7096	1.7098	-0.0001
0 4 1	54.359	54.334	0.025	1.6863	1.6870	-0.0007
2 4 0	54.899	54.964	-0.065	1.6710	1.6692	0.0018
4 2 0	55.512	55.434	0.078	1.6540	1.6561	-0.0021
1 4 1	55.884	55.774	0.110	1.6439	1.6468	-0.0030
3 3 1	57.730	57.864	-0.134	1.5956	1.5922	0.0034
2 2 2	59.363	59.283	0.079	1.5556	1.5575	-0.0019
2 4 1	60.306	60.364	-0.057	1.5335	1.5321	0.0013
4 2 1	60.884	60.743	0.141	1.5203	1.5235	-0.0032
3 4 0	62.235	62.014	0.221	1.4905	1.4953	-0.0048
4 3 0	62.566	62.483	0.083	1.4834	1.4852	-0.0018

Refined cell:  $a = 7.372(5) \text{ \AA}$ ,  $b = 7.499(5) \text{ \AA}$ ,  $c = 3.860(3) \text{ \AA}$ ,  $V = 213.4 \text{ \AA}^3$ . Agreement:  $|\Delta(2\theta)| = 0.07^\circ$ ,  $|\Delta(d)| = 0.004 \text{ \AA}$ , ESD of fit =  $0.08^\circ$  (ESD, estimated standard deviation).

## References

- [1] M.T. Pope, Heteropoly and Isopoly Oxometalates, Springer, Berlin, New York, 1983.
- [2] C.L. Hill (Ed.), Polyoxometalates (special issue), Chem. Rev. 98 (1998) 1–389.
- [3] M.T. Pope, in: J. McCleverty, T.J. Meyer (Eds.), Comprehensive Coordination Chemistry II, vol. 4, Pergamon Press, Oxford, 2004, pp. 635.
- [4] C.L. Hill, in: J. McCleverty, T.J. Meyer (Eds.), Comprehensive Coordination Chemistry II, vol. 4, Pergamon Press, Oxford, 2004, pp. 679.
- [5] A. Besserguenev, M.H. Dickman, M.T. Pope, Inorg. Chem. 40 (2001) 2582.
- [6] K. Wassermann, M.T. Pope, M. Salmen, J.N. Dann, H.-J. Lunk, J. Solid-State Chem. 149 (2000) 378.
- [7] C.J. Besecker, V.W. Day, W.G. Klemperer, M.R. Thompson, Inorg. Chem. 24 (1985) 44.
- [8] F. Ortega, M.T. Pope, Inorg. Chem. 23 (1984) 3292; (b) H. Kwen, S. Tomlinson, E.A. Maatta, C. Dablemont, R. Thouvenot, A. Proust, P. Gouzerh, Chem. Commun. (2002) 2970; (c) C. Dablemont, A. Proust, R. Thouvenot, C. Afonso, F. Fournier, J.-C. Tabet, Inorg. Chem. 43 (2004) 3514.
- [9] A. Venturelli, M.J. Nilges, A. Smirnov, R.L. Belford, L.C. Francesconi, J. Chem. Soc. Dalton Trans. (1999) 301.
- [10] F. Ortega, M.T. Pope, H.T. Evans Jr., Inorg. Chem. 36 (1997) 2166.
- [11] M.J. Abrams, C.E. Costello, S. Shaikh, J. Zubietta, Inorg. Chim. Acta 180 (1991) 9.
- [12] B.N. Ivanov-Emin, D.K. Chakrabarti, A.E. Ezhov, Russ. J. Inorg. Chem. 11 (1966) 733 (Engl. Trans.).
- [13] C. Tourné, A. Revel, G. Tourné, M. Vendrell, C.R. Acad. Sci. Ser. C 273 (1973) 643.
- [14] J. Mialane, E. Marrot, J. Rivière, G. Nebout, G. Hervé, Inorg. Chem. 40 (2001) 44.
- [15] Y. Jeannin, J. Martin-Frère, J. Am. Chem. Soc. 103 (1981) 16.
- [16] A.W. Sleight, J.L. Gillson, Solid-State Commun. 4 (1966) 601.
- [17] K. Okada, H. Morikawa, F. Marumo, S. Iwai, Acta Crystallogr. Ser. B B32 (1976) 1522.
- [18] A. Magneli, Acta Chem. Scand. A 11 (1957) 28.
- [19] J.E. Schirber, B. Morosin, R.W. Alkire, A.C. Larson, P.J. Ver-gamini, Phys. Rev. B29 (1984) 4150.
- [20] B. Krebs, A. Muller, H.H. Beyer, Inorg. Chem. 8 (1969) 436.
- [21] R. Nedjar, M.M. Borel, M. Hervieu, B. Raveau, Mater. Res. Bull. 23 (1988) 91.
- [22] B. Gerand, G. Nowogrocki, J. Guenot, M. Figlarz, J. Solid-State Chem. 29 (1979) 429.
- [23] K. Kihlborg, A. Hussain, Mater. Res. Bull. 14 (1979) 667.
- [24] P.G. Dickens, R.J. Hurditch, Nature 215 (1967) 1266.
- [25] P. Hagenmuller, in: J.C. Bailar Jr., H.J. Emeléus, R. Nyholm, A.F. Trotman-Dickenson (Eds.), Comprehensive Inorganic Chemistry, vol. 4, Pergamon Press, Oxford, 1973, pp. 549.
- [26] B.O. Loopstra, H.M. Rietveld, Acta Crystallogr. Ser. B B25 (1969) 1420.
- [27] E. Salje, Acta Crystallogr. Ser. B B33 (1977) 574.